Dalton Transactions

Accepted Manuscript

ROYAL SOCIETY OF CHEMISTRY

www.rsc.org/dalton

Dalton Transactions

Dynamic Article Links ►

Cite this: DOI: 10.1039/c0xx00000x

www.rsc.org/xxxxxx

ARTICLE TYPE

Synthesis and Characterization of Bis (acetylacetonato κ-O, O') [zinc (II)/copper (II)] Hybrid Organic-inorganic Complexes as Solid Metal Organic Precursor

Reza Rooydell,[a] Ruey-Chi Wang,[b] Sanjaya Brahma,[c] Farzaneh Ebrahimzadeh,[d] Chuan-Pu Liu[a]*

Received (in XXX, XXX) Xth XXXXXXXXX 20XX, Accepted Xth XXXXXXXXX 20XX

DOI: 10.1039/b000000x

We have synthesized novel metal organic hybrid mixed compounds of bis (acetylacetonato κ-O, O') [zinc (II)/copper (II)]. Taking $C_{10}H_{14}O_4Zn_{0.7}Cu_{0.3}$ ($Z_{0.7}C_{0.3}AA$) as an example, the crystals are composed of $Z_{0.7}C_{0.3}AA$ units and uncoordinated water molecules. Single-crystal X-ray diffraction results show that the complex $Z_{0.7}C_{0.3}AA$ crystallizes in the monoclinic system, space group $P2_1/n$. The unit cell dimensions are a = 10.329(4) Å, b = 4.6947(18) Å, and c = 11.369(4) Å; the angles are α = 90°, β = 91.881(6) °, and γ = 90°, the volume is 551.0(4) Å^3, and Z = 2. In this process, the M (II) ions of Zn and Cu mix and occupy the centers of symmetrical structure units, which are coordinated to two ligands. The measured bond lengths and angles of O-M-O vary with the ratio of metal species over the entire series of the complexes synthesized. The chemistry of the as-synthesized compounds has been characterized using infrared spectroscopy, mass spectroscopy, energy-dispersive X-ray spectroscopy, and X-ray photoelectron spectroscopy analysis, and the morphology of the products has been characterized using scanning electron microscopy. The thermal decomposition of the $Z_{0.7}C_{0.3}AA$ composites measured by thermo gravimetric analysis suggests that these complexes are volatile. The thermal characteristics of these complexes make them attractive precursors for metal organic chemical vapor deposition.

Introduction

The synthesis of hybrid organic-inorganic materials has been the subject of intensive research[1-8] due to their interesting structural chemistry and potential applications in areas such as ion exchange, adsorption, and catalysis[9-11]. Compared to monometallic complexes, metal organic hybrid complexes have more varied compositions and crystal structures, and thus more diversified properties and applications[12]. Metal-organic (MO) complexes have been widely employed as precursors for the growth of various thin films and nanostructures using chemical vapor deposition (CVD)[13,14]. Along the way, it is also of further interest to synthesize solid solutions of metal acetylacetonates[15], so that growth of multi-element compound crystalline materials via simple growth route with control in compositions could be achieved. By taking this growth route, growth evolution into thin films or nanomaterials maybe easily controlled with precision in composition. Bi-metal complex acetylacetonates characterized in this manner could be employed for the preparation of compound oxides by CVD[16]. The compound or doped oxide would form an interesting set of semiconductors with electronic and optical properties variable from various compositions or dopants.

One of the most common ligands for the formation of transition metal complexes is acetylacetone ($C_5H_8O_2$, AA) (2,4-Pentandione), which is a bidentate ligand that chelates to metal atoms through two oxygen atoms in a six-membered ring[17-20]. Paired with this ligand, zinc acetylacetonate (ZAA) and copper acetylacetonate (CAA) complexes can be applied to promote CVD growt[21-23], as Lewis acids in coordination chemistry[24], and in the formation of inorganic polymers[25]. Several strategies for the preparation of various MO precursors have been reported in previous studies. However, some of these methods suffer from serious drawbacks, such as low product yield, rapid increase of pH during reactions, the use of expensive and dangerous chemicals, long reaction times, inconvenience in handling, and restrictions in the choice of metal species.

Formation of hydrogen bonding in MO complexes is an issue in stabilization of the structure, since carbon is generally not considered as a conventional hydrogen bond donor due to its relatively low electronegativity compared with oxygen and nitrogen. However, several studies have shown that even aliphatic carbon atoms are capable of forming weak hydrogen bonds, denoted as C–H···O hydrogen bonds, or C–H···A, where A is acceptor from (O, N, F), and (C···H)π being intermolecular interactions wherein a hydrogen atom forms a bond between two structural moieties of C and A[26-29]. The most commonly used method for revealing hydrogen bond interactions is to examine the hydrogen bond length between the donor and acceptor groups. The distances between atoms that are equal or less than that of the sum of the atoms van der Waals radii often indicate hydrogen bond formation[30].

Hybrid Zn/Cu complexes are technically interesting but seldom reported. In this research, we attempt to synthesize Zn/Cu bimetallic complex with AA to act as a MO precursor, with

Zn/Cu atoms being four-coordinated. Here, we report a facile method for the formation of crystalline bis (acetylacetonato κ-O, O') [Zn (II)/Cu (II)] complex (ZCAA) via two methods: (1) reactions of Zn $(NO_3)_2{\cdot}6H_2O$ and Cu $(NO_3)_2{\cdot}3H_2O$ and (2) reactions of ZAA and CAA in EtOH/H_2O (EtOH-ethanol). Synthesis parameters such as the concentrations of Zn/Cu initiators, pH, and temperature are found to be important in the preparation of this bimetallic complex, in which the two metals occupy the center positions. For better understanding on the formation of H bonding, the atomic structures of these compounds are examined by single crystal X-ray diffraction.

The mixed-metal acetylacetonate complex containing zinc and copper [$Zn_{0.7}Cu_{0.3}$AA] synthesized in this work has been used to prepare nanoparticles, nanowires and thin films of the mixed zinc-copper metal oxides, ($Zn_{1-x}Cu_x$) O, which will be published elsewhere. These complexes facilitate the formation of oxides with various compositions and doping concentrations in uniform distribution because of the existence of the direct bonds between metal and oxygen as well as between different types of metals in the molecular structure. Consequently, one can avoid the complications involving additional chemical reactions during the formation of compound oxides that would happen if two metal compounds having different vapor pressure are used by a similar growth process. The authors have demonstrated the deposition of thin film oxides using metal acetylacetonates as ''single-source'' precursors for the growth of the compound oxides. This is the initiative to synthesize such complexes that involve both the metals Zn and Cu.

Experimental procedure

All the chemicals used here are analytical grade, purchased from Merck and Fluka. Solvents were purified using standard procedures wherever required. The synthesis procedures for complexes with various atomic ratios of Zn to Cu are identical.

The procedure used for preparing the complex containing 70% Zn and 30% Cu, $C_{10}H_{14}O_4Zn_{0.7}Cu_{0.3}$AA ($Z_{0.7}C_{0.3}$AA), may be given as an example from the series of compounds with various ratios of Zn to Cu. Copper nitrate 30% (1 mmol, 0.242 g) dissolved in 10 ml EtOH/H_2O (30%) was added slowly to a solution of zinc nitrate (1 mmol, 0.295 g) in 40 ml EtOH/H_2O (30%), and then mixed by magnetic stirring for 10 min. Then, AA (2.05 ml) in EtOH/H_2O (30%, 50 ml) was added drop by drop to the mixture over a period of 10 min, after which the mixture was heated to 60 °C for 30 min. The pH value of the mixture was then adjusted to 5.5-6.5 using KOH solution (1.5 M in EtOH/H_2O (30%) using a pH meter. The mixture was then heated for one more hour at 60 °C. Subsequently, precipitates were collected after being filtered out and rinsed with a mixture of water and ethanol at EtOH/H_2O (30%) to remove unreacted materials. The as-synthesized complexes were then recrystallized in EtOH for further purification to obtain shiny and needle-like crystals, which were finally air-dried. Alternatively, Zn $(NO_3)_2$ and Cu $(NO_3)_2$ can be replaced by ZAA and CAA, respectively, as the starting materials, and identical crystalline products will be produced. Bimetallic complexes with various composition ratios can be derived by adjusting the molar ratio of Zn to Cu in the starting recipe. The overall yield was found to be ~85%. The product could easily be re-dispersed in polar organic solvents, such as EtOH, and mixed of EtOH/H_2O. At room temperature, the solubility is low but the solubility increases with increase of temperature.

Mass spectroscopic data were recorded using a JEOL spectrometer (MStation JMS700). The crystal structure was analyzed through X-ray diffraction (XRD) using a Bruker AXE D8 GADDS micro diffractometer. Single crystal data of $C_{10}H_{14}Cu_{0.30}Zn_{0.70}O4$ [$Z_{0.7}C_{0.3}$AA] was collected at 296(2) K by employing a "Bruker Smart" diffractometer equipped with CCD area-detector and Mo Kα radiation (λ = 0.71073 Å). The data is refined by using SHELXL-97 [26]. The final R1 = 0.0323, and wR2 = 0.0779 with goodness-of fit on F^2 of 1.052. Table 3 summarizes the details about the crystal structure data of $Z_{0.7}C_{0.3}$AA complex. Further details about the crystallographic data could be obtained from Cambridge Crystallographic Data Centre (CCDC 981571).

The chemical composition was identified using an energy-dispersive X-ray spectroscopy (EDX) detector on a scanning electron microscope (SEM; HITACHI SU 8000) and a transmission electron microscope (TEM; JEOL 2100F). The chemical bonding was examined using X-ray photoelectron spectroscopy (XPS; VG ESCA-210D). The composition was confirmed using thermogravimetric analysis (TGA; Setaram TG92), performed up to 400 °C under helium flow. The functional groups of ligands and complexes were analyzed by Fourier transform infrared (FT-IR) spectroscopy on an FT-IR Nicolet 5700 spectrometer (Thermo Electron Corporation) using KBr disks in the range of 400-4000 cm^{-1}.

Results and discussion

The luster of the as-syntheiszed needle-like $Z_{0.7}C_{0.3}$AA crystals is directly related to the amount of Cu in the complex. The color ranges from deep blue for Cu $(acac)_2$ (Fig 1(a)) to light blue for $Z_{0.7}C_{0.3}$AA (Fig. 1(b)). The diameter and length of the needles are around 14-20 and 400-970 μm, respectively. Figure 1(c) shows a SEM image of the $Z_{0.7}C_{0.3}$AA crystals, revealing their morphology as micro-needles with a length of 400-950 μm and a diameter of 14-20 μm. After two days of recrystallization, these aggregates transform into smooth rods with an average length of approximately 800 μm and a diameter of 6 μm.

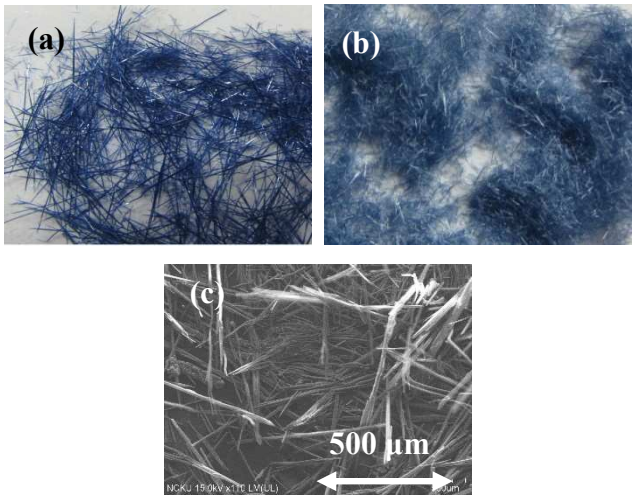

Fig. 1. Optical microscopy images of (a) CAA and (b) $Z_{0.7}C_{0.3}$AA. (c) SEM image of $Z_{0.7}C_{0.3}$AA.

Figure 2(a) shows a low magnification TEM image of typical ZCAA needle-like products. The image in Fig. 2(b) is taken at medium magnification from a thin area in Fig. 2(a); revealing that the ZCAA needle is made of chessboard webs, where long fibers are inter-woven with highly oriented long-chain crystals self-assembled in a manner which connects the two neighboring fibers to form networks with a lot of voids. The

close-up TEM image in Fig. 2(c) shows long chains made of tiny particles imbedded in an amorphous matrix.

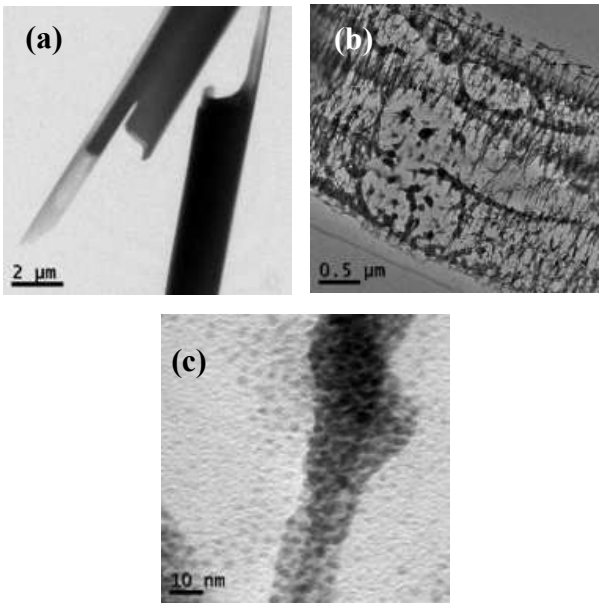

Fig. 2. TEM analysis of typical ZCAA needle-like products: (a) low magnification image, (b) medium magnification image of a thin area in (a), (c) high magnification image of a typical chain in (b).

During synthesis, the driving force behind the incorporation of Zn and Cu ions in acac into $Z_{0.7}C_{0.3}AA$ crystal lattices is hydrogen bond formation, as illustrated in Fig. 3. The complex can only be synthesized under optimal growth conditions (temperature and pH). The optimal temperature is in the range of room temperature to 80 °C. The highest yield is obtained at a pH value of 5-7. As shown in Fig. 3, acac undergoes keto-enol isomerization, resulting in a mixture of two tautomers at room temperature. The hydroxylic proton is easily ionized and the negative charge in the resulting anion is delocalized over the molecule. Basic (acidic) conditions promote the enolic (keto) form; only neutral conditions allow both forms to co-exist.

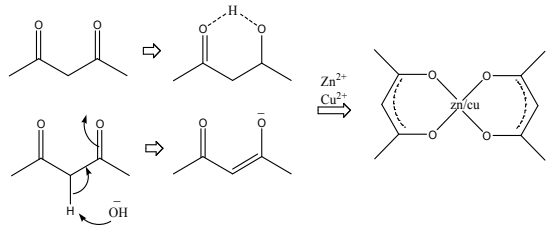

Fig. 3. Proposed reactions for $Z_{0.7}C_{0.3}AA$ formation

EDX analysis is performed to determine the composition of the new compound. Figure 4 shows that the sharp Kα signals of Cu and Zn confirm the presence of Zn and Cu in this homogenous crystal. The atomic ratio of Zn:Cu:O is about 15.1:7.4:77.5, which is close to the nominal composition in the starting materials. EDX analysis reveals that the atomic ratio of Zn to Cu is about 2 to 1, and that of O to M (Zn+Cu) is around 4 to 1, suggesting that every metal is surrounded by 4 oxygen atoms, which is consistent with the atomic structure model in Figure. 3. The composition has also been confirmed by inductively coupled plasma mass spectra (not shown).

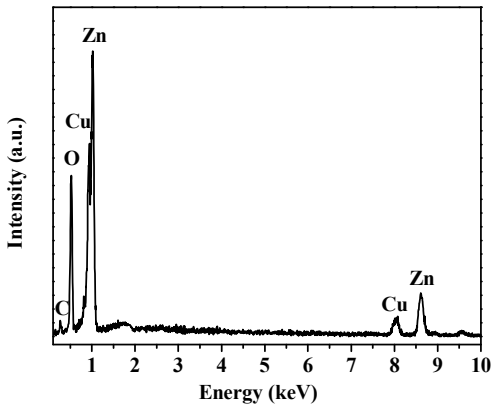

Fig. 4. EDX spectrum of $Z_{0.7}C_{0.3}AA$ compound.

The IR spectra of the as-synthesized ZAA, CAA, and $Z_{0.7}C_{0.3}AA$ in the range of (a) 400-1000 cm^{-1}, (b) 950-1800 cm^{-1} shown in Fig. 5 contain metal and non-metal groups.[1-2] The detailed assignments of the peaks for the three samples are shown in Table 1. By comparing with the FTIR spectra of ZAA and CAA, the peaks at 428 cm^{-1}, 557 cm^{-1} and 771 cm^{-1} are exclusively characteristics of ZAA in ZCAA. Therefore, the spectrum of the compound complex with higher Zn concentration is more akin to ZAA. The FT-IR spectrum of $Z_{0.7}C_{0.3}AA$ in Fig. 5 can be divided into three main regions. The first region, between 3200 and 2600 cm^{-1}, contains the C-H stretching vibrations of several methyl and methylene groups of acac. The second region, between 1800 and 1000 cm^{-1}, contains the stretching vibrations of the C=O and C=C groups, and the bending and rocking modes of the C-H groups. The υC=O mode appears at 1597, 1578, and 1600 cm^{-1} for ZAA, CAA, and $Z_{0.7}C_{0.3}AA$, respectively. The FT-IR spectra of ZAA, CAA, and $Z_{0.7}C_{0.3}AA$ powders all show two composite peaks in the 1250-1600 cm^{-1} region, assigned to the C-O-M bonds. These composite peaks are caused by delocalized electrons in the C-O-M bonds, which are found only in the acac bidendate mode, suggesting that the acac-M bonds in these powders are probably all bidendate. The third region, between 1000 and 400 cm^{-1}, includes the stretching vibrations of the C-CH_3, Zn-O, and Cu-O bonds, as well as the symmetric bending modes of the C-H groups. For the metal-ligand (M-L) bond group, copper-ligand (Cu-L) and Cu-O appear at 430 and 454 cm^{-1}, respectively, for CAA, whereas zinc-ligand (Zn-L) and Zn-O appear at 420 and 555 cm^{-1}, respectively, for ZAA; Zn-L and Cu-L appear at 428, for $Z_{0.7}C_{0.3}AA$. The peaks from $Z_{0.7}C_{0.3}AA$ are contributed by both Zn and Cu, with a slight shift relative to CAA and ZAA due to the co-existence of Zn and Cu in one complex. The peaks at 653 (ZAA) and 685 cm^{-1} (CAA) correspond to ring def and ring def+ υ (M-L), respectively, which also appear in $Z_{0.7}C_{0.3}AA$, reassuring the presence of both Zn and Cu atom in the complex.

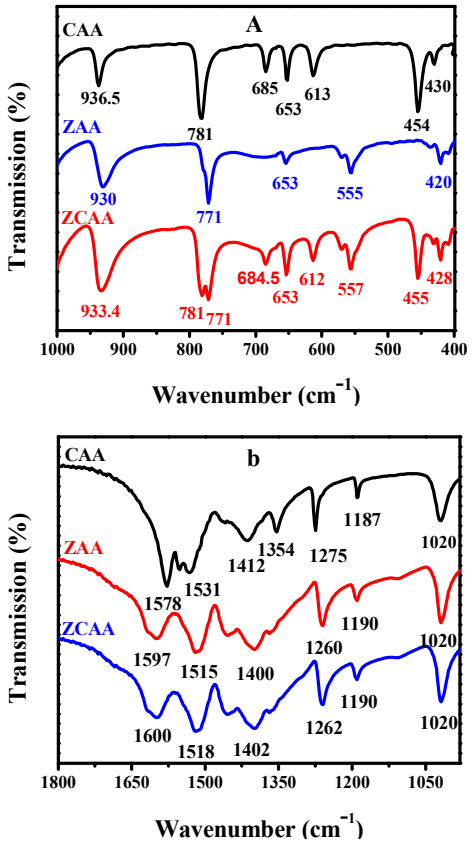

Fig. 5. FT-IR spectra of ZAA, CAA, and $Z_{0.7}C_{0.3}AA$ in (a) 400-1000 cm^{-1}, (b) 950-1800 cm^{-1}.

Table 1 Assignments of the peaks in the FT-IR spectra of CAA, ZAA, and $Z_{0.7}C_{0.3}AA$.

Assignment	CAA	ZAA	$Z_{0.7}C_{0.3}AA$
υ (M-L) ring def.	430(cm^{-1})	420(cm^{-1})	428(cm^{-1})
υ (M-O) ring def.	454(cm^{-1})	555(cm^{-1})	455(cm^{-1}) 557(cm^{-1})
ring def. + υ (M-L)	685(cm^{-1})	653(cm^{-1})	684 (cm^{-1})
υ (C-CH & + ν(C=O)	937(cm^{-1})	930(cm^{-1})	933.5(cm^{-1})
υ (C-C) + ν(C-CH_3)	1274(cm^{-1})	1260(cm^{-1})	1262(cm^{-1})
υ (C=C)	1531(cm^{-1})	1515(cm^{-1})	1518(cm^{-1})
υ (C=O)	1578(cm^{-1})	1597(cm^{-1})	1600(cm^{-1})

In mass spectroscopy measurements, the compound is ionized by electrons inside the mass spectrometer. Figure 6 shows all possible fragments for $Z_{0.7}C_{0.3}AA$, including mass/charge ratios, which should be present in the mass spectra as distinct signatures of the chemical bonding in $Z_{0.7}C_{0.3}AA$.The mass spectrum of $Z_{0.7}C_{0.3}AA$ is shown in Fig. 7. The molecular weight of ZAA is 263 g/mol, and CAA is 261 g/mol, giving rise to peaks at 263 m/z and 261 m/z, respectively, which then reduce to 164 m/z and 162 m/z when one molecule of AA (acac) is removed, followed by 63 m/z and 65 m/z, for Cu and Zn, respectively, when two molecules of acac are removed. The presence of these peaks indicates the presence of CAA and ZAA, which might be dissociated from the $Z_{0.7}C_{0.3}AA$ complex.

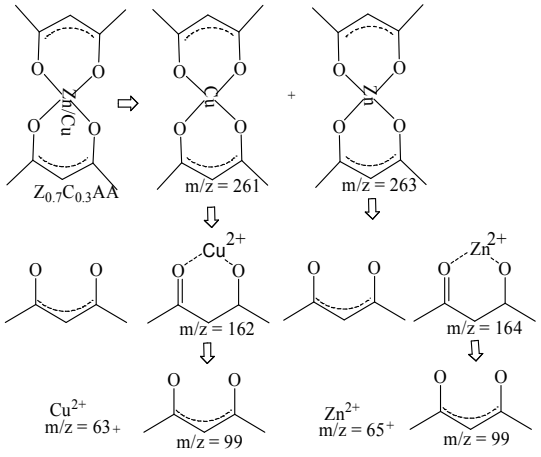

Fig. 6. Mass fragments of $Z_{0.7}C_{0.3}AA$.

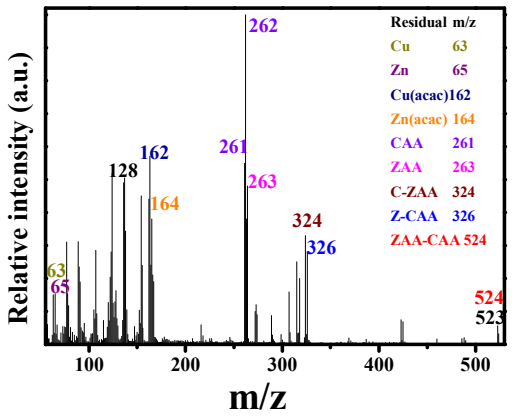

Fig.7. Mass spectrum of $Z_{0.7}C_{0.3}AA$

The chemical states of Zn, Cu, O, and C in $Z_{0.7}C_{0.3}AA$ can be studied by XPS in Fig. 8. The binding energy scale for each element has been calibrated using the adventitious carbon peak (C-1s) at 284.73 eV. In addition to this peak, the C-1s spectrum of the $Z_{0.7}C_{0.3}AA$ complex in Fig. 8(d) exhibits peaks at 286.6 and 288.7 eV, corresponding to C=O. Moreover, the spectrum shows peaks at 1021.79 eV ($2p_{3/2}$) and 1044.8 eV ($2p_{1/2}$) for Zn, as well as peaks at 933.22 eV ($2p_{3/2}$) and 953.11 eV ($2p_{1/2}$) for Cu, confirming that both Cu and Zn atoms serve as the main

metallic elements of the complex. Interestingly, both Zn and Cu doublet peaks exhibit chemical shifts compared with their counterparts from ZAA and CAA, as shown in Table 2. By changing the chemical nature from ZAA through the insertion of more Cu into the surrounding Zn, the Zn doublets are shifted toward higher binding energies by 0.16 eV, while the Cu doublets are shifted toward lower binding energies by 1.08 eV from CAA to $Z_{0.7}C_{0.3}AA$. Finally, the asymmetric peak observed in the O 1s spectrum in Fig. 8(c) at 531.7 eV contains different oxygen origins into several sub-spectral components, as (i) O in defective ZnO_x and/or ZnOH at 531.7 eV, (ii) adventitious O in CO at 531.1 eV, (iii) adventitious O in CO_2 at 532.5 eV, and (iv) O around Zn affected by Cu presence at 537 eV[8].

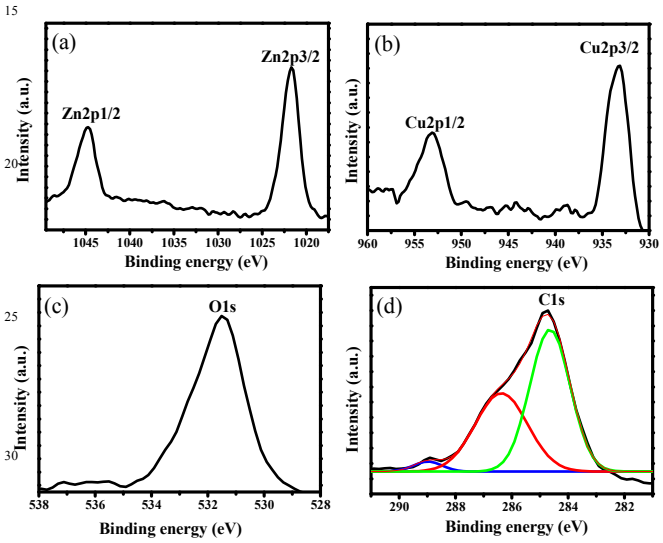

Fig. 8. XPS spectra of $Z_{0.7}C_{0.3}AA$ for (a) Zn 2p, (b) Cu 2p, (c) O 1s, and (d) C 1s

Table 2: XPS results for Zn and Cu doublet peaks for CAA, ZAA, and $Z_{0.7}C_{0.3}AA$

Sample	O 1s	Zn $2p_{3/2}$, $2p_{1/2}$	Cu $2p_{3/2}$, $2p_{1/2}$
CAA	531.58	-	934.3-954.2
ZAA	531.59	1021.63-1044.64	-
ZCAA	531.49	1021.79-1044.80	933.22-953.11

Figure 9 shows XRD patterns of ZCAA complexes with nominal Cu compositions of 10%, 30%, and 50%. The diffraction peaks reveal the same features for all the complexes, implying that they belong to the same monoclinic phase. The sharp diffraction peaks suggest a high degree of crystallinity for all the as-prepared complexes. The peak positions shift toward higher angle as the Cu composition increases. For example, the (101) peak shifts from 11.41° to 11.49° and further to 11.56° when the Cu composition increases from 10% to 30% to 50%, respectively. Correspondingly, the d spacing of the (101) plane decreases from 7.745 to 7.696 to 7.649 Å, respectively, which is consistent with the replacement of larger Zn ions with smaller Cu ions in the complex.

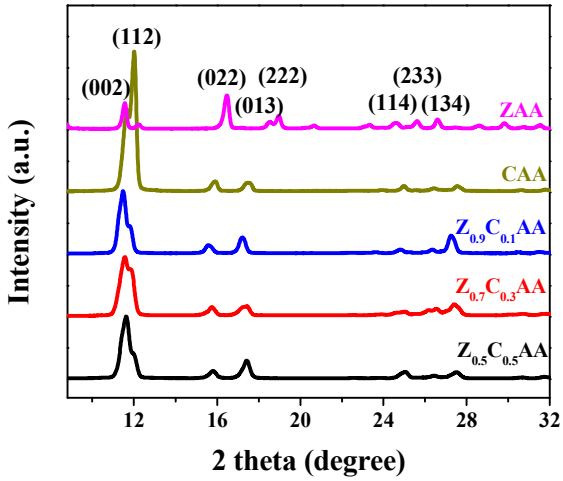

Fig. 9. XRD patterns of ZCAA complexes with Cu compositions of (a) ZAA, (b) CAA, (c) 10%, (d) 30%, and (e) 50%.

The crystal structure of $Z_{0.7}C_{0.3}AA$ shown in Fig. 10 is refined further by analyzing the single-crystal XRD patterns acquired from single-crystalline particles, where (a) is the structure of one molecule, while (b) and (c) exhibit unit cells containing 9 such molecules but viewed along the b and c direction, respectively. As shown in Fig. 10 (a), the coordination geometry around Zn (II)/Cu (II) is square, with the basal plane defined by four O atoms from two chelating acac ligands. This complex crystallizes in the monoclinic phase with space group $P2_1/n$, consistent with the results derived from the XRD patterns shown in Fig. 9. The unit cell dimensions are: a = 10.329(4) Å, b = 4.6947(18) Å, and c = 11.369(4) Å; the angles are: α = 90°, β = 91.881(6)°, and γ = 90°; the volume is 551.0(4) $Å^3$. The unit cell dimensions (a, b, c), angles (α, β, γ), and volume of $Z_{0.7}C_{0.3}AA$ are divergent from those of ZAA and CAA, even though they belong to the same monoclinic phase, due to the size difference between Cu and Zn. Table 3 summarizes the crystallographic data of $Z_{0.7}C_{0.3}AA$ complex.

A detailed comparison of the unit cell structures among $Z_{0.7}C_{0.3}AA$, ZAA, and CAA is given in Table 4. For ZAA, the space group is $P2_1$; the unit cell dimensions are: a = 10.411(3) Å, b = 5.3571(16) Å, and c = 10.873(3) Å; the angles are: α = 90°, β = 93.199(5)°, and γ = 90°; the volume is 605.5(3) $Å^3$. For CAA, the space group is $P2_1/n$; the unit cell dimensions are: a = 10.336(4) Å, b = 4.6980(17) Å, and c = 11.387(4) Å; the angles are: α = 90°, β = 91.829(6)°, and γ = 90°; the volume is 552.6(3) $Å^3$. In $Z_{0.7}C_{0.3}AA$, Zn/Cu metals are coordinated with two acac ligands and bonded to four oxygen atoms of acac. Each acac acts as a bidentate ligand bonded to the cationic ion through its carbonyl oxygen atom, resulting in a crystallographically planar configuration of ZnO_4, CuO_4.

Table 3 Crystal data of $Z_{0.7}C_{0.3}AA$

Empirical formula	$C_{10}H_{14}Zn_{0.70}O_4Cu_{0.30}$
Formula weight	259.82
Temperature	296(2) K
Wavelength	0.71073 Å
Crystal system	Monoclinic
Space group	$P2_1/n$
Unit cell dimensions	a = 10.329(4) Å α= 90°
	b = 4.6947(18) Å β= 1.881(6)°
	c = 11.369(4) Å γ = 90°
Volume	551.0(4) $Å^3$
Z	2
Density (calculated)	1.566 Mg/m^3
Absorption coefficient	2.044 mm^{-1}
Crystal size	0.97 x 0.02 x 0.014 mm^3
collection Reflections collected	3905
Independent reflections	1356 [R(int) = 0.0265]
Absorption correction	Semi-empirical from equivalents
Max. and min. transmission	0.7457 and 0.6005
Refinement method	Full-matrix least-squares on F^2
Goodness-of-fit on F^2	1.052
Final R indices [I>2sigma(I)]	R1 = 0.0323, wR2 = 0.0779
R indices (all data)	R1 = 0.0507, wR2 = 0.0872
Largest diff. peak and hole	0.272 and -0.309 $e.Å^{-3}$

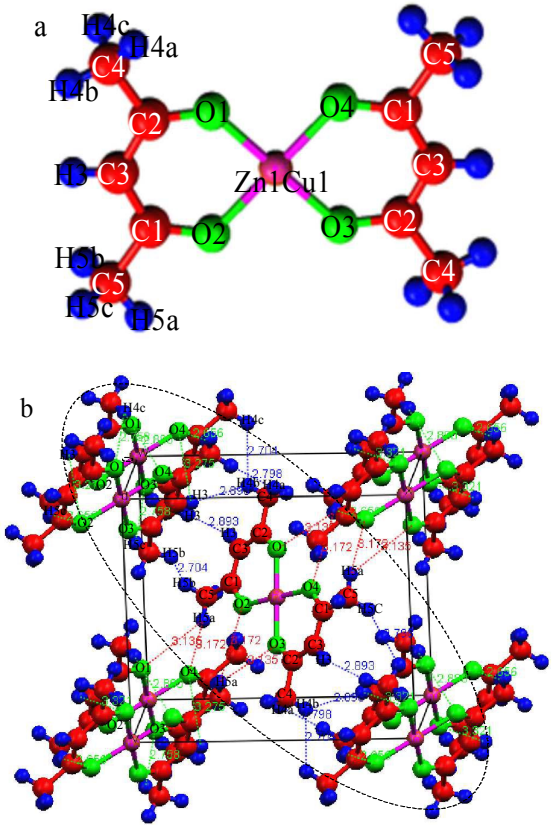

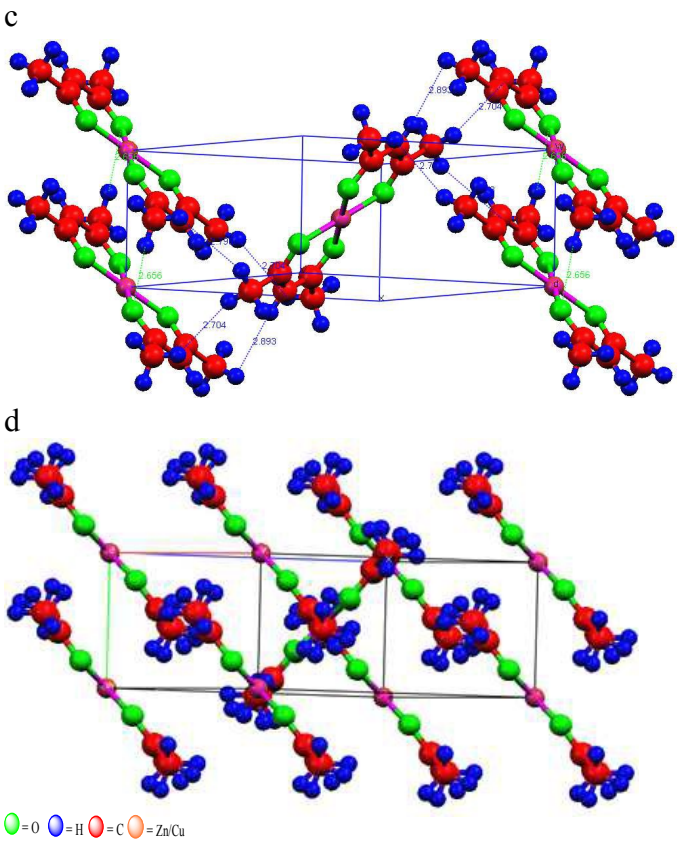

Fig. 10. $Z_{0.7}C_{0.3}AA$ molecular packing diagrams: (a) molecular configuration (b,c,d) molecular packing into a unit cell view along the b and c direction respectively.

Fig.10 (b) shows molecular packing into the unit cell diagram of $Z_{0.7}C_{0.3}AA$, where the molecules occupying the center and corner positions of the unit cell share the same structure but with different orientations. In this unit cell constructed by 1 molecule at the center and 8 molecules at the corners, there are three different atomic coordinations involving H bonding, through which the unit cell can be compacted, including (C–H···O), (C–H···O) π and (H···H) covalent bonding denoted by red, green and blue, respectively. The first group of (C–H···O) bonding in red is located between the center O atom and corner molecules (C-H group), such as C3H3···O1 = 3.27 Å, C4H4a…O2 = 3.135 Å and C4H4a…O3 = 3.172 Å. The second group of (C–H···O) π bonding in green involves C-H from two molecules at the corners of the unit cell with the bond length shorter than (C–H···O) bonding in Fig. 10 (b), such as C4H4b···O1 = 2.65 Å, C5H5c···O4 = 2.75 Å, C3H3···O1 = 3.27 Å, C4H4a…O2 = 3.135 Å, and C4H4a…O3 = 3.172 Å. The third group of (H···H) covalent bonding connects the center with corner molecules through H atoms from each molecule, as denoted by blue color in Fig. 10(b) and (c). The (H···H) bonding lengths are varied between 2.7-2.9 Å[17,18]. The complete H bonding list with bond lengths are referred in Fig. 10 and Table 4. The single crystal X-ray diffraction results show that the bond angle and bond length of (C–H···O) in ZCAA fall in the range of (106-150°) and (2.6-3.2 Å) respectively, where significantly different orientations exist between the acac in the center and corner of ZCAA. The (C–H···O) interactions play an important role in metal-organic systems, especially in the ZCAA ligands to make the structure more stabilized.

The bond lengths and angles of other non-H bonds in CAA, ZAA, and $Z_{0.7}C_{0.3}AA$ are compared in Tables 5 and 6. The symbols are defined in Fig. 10. Due to the mismatch in size between Zn and Cu, a partial substitution of Zn with Cu in the $Z_{0.7}C_{0.3}AA$ complex leads to different bond lengths and angles in the unit cells of the same parent phase.

Table 4. Bond lengths of different (C–H···O), (C–H···O) π and (H···H) bonding in the unit cell of $Z_{0.7}C_{0.3}AA$

Atomic bonding	Type of bond	Bond length(A°) t(bond length)
C4H4b-O1	(C–H···O) π	2.656
C5H5c-O4	(C–H···O) π	2.758
C4H4a-O1	(C–H···O)	3.135
C4H4a-O4	(C–H···O)	3.172
C3H3-O1	(C–H···O)	3.275
C3H3-O2	(C–H···O)	3.321
C4H4C-C5H5b	(H···H)	2.70
C5H5a-C4H4c	(H···H)	2.79
C3H3-C5H5b	(H···H)	2. 80

Table 5. Comparison of bond lengths in the unit cells of CAA, ZAA, and $Z_{0.7}C_{0.3}AA$

	CAA (Å)	ZAA (Å)	$Z_{0.7}C_{0.3}AA$(Å)
M- O_1	1.924	2.017	1.917
M-O_2	1.918	2.032	1.9191
M-O_3	1.924	2.032	1.9174
M-O_4	1.918	2.017	1.9191
O_1-C_2	1.272	1.265	1.278
O_2-C_1	1.272	1.277	1.272
C_1-C_3	1.388	1.384	1.390
C_2-C_3	1.385	1.387	1.387
C_2-C_4	1.502	1.515	1.499
C_1-C_5	1.5	1.512	1.505

Table 6. Comparison of bond angles in the unit cells of CAA, ZAA, and $Z_{0.7}C_{0.3}AA$.

	CAA(°)	ZAA (°)	$Z_{0.7}C_{0.3}AA$ (°)
O_1-M-O_2	93.5	88.37	93.65
O_1-M-O_4	86.5	84.35	86.35
O_1-M-O_3	180	180	180
O_2-M-O_3	86.5	84.35	86.35
O_2-M-O_4	180	180	180
M-O_1-C_2	125.4	127.1	125.4
M-O_2-C_1	125.37	126.4	125.37
O_1-C_2-C_3	124.9	125	124.8
O_2-C_1-C_3	125	125	125

The TGA results of the three hybrid metal organic complexes of $Z_{0.85}C_{0.15}AA$, $Z_{0.7}C_{0.3}AA$, $Z_{0.55}C_{0.45}AA$ along with ZCC and CAA are shown in Fig.11. As for the complex of $Z_{0.85}C_{0.15}AA$, the weight loss is nearly 1% up to 159 °C and then increases rapidly to about 88% at 235 °C. A 3% weight loss occurs at about 175 °C, implying that this complex can be used as a precursor around this temperature in a practical CVD process for the deposition of compounds containing these two elements, such as Cu doped ZnO thin films. The other two complexes of $Z_{0.7}C_{0.3}AA$, $Z_{0.55}C_{0.45}AA$ exhibit similar behavior to that of $Z_{0.85}C_{0.15}AA$, however, the decomposition temperature slightly increases with the Cu composition in the complex. The temperature for the 3% weight loss increases to 178 °C for $Z_{0.7}C_{0.3}AA$, and 182 °C for $Z_{0.55}C_{0.45}AA$. Notably, the decomposition temperature of the hybrid complexes is higher than that of the two parent compounds, where CAA is still similar but ZAA exhibits a large deviation from the trend. Therefore, compared to ZAA (162 °C) and CAA (232 °C), the initial weight loss of the hybrid complexes is minimal, implying greater thermal stability. The TGA of ZAA shows two step decompositions: one at ~60 °C that corresponds to initial mass loss due to the evaporation of the absorbed moisture. The second step mass loss within 60 - 160 °C is attributed to the decomposition of the ZAA complex. The TGA spectra demonstrates that all the complexes can be decomposed in one single step and so can be considered to be promising starting precursor materials for the growth of thin films or nanomaterials with tunable compositions by CVD.

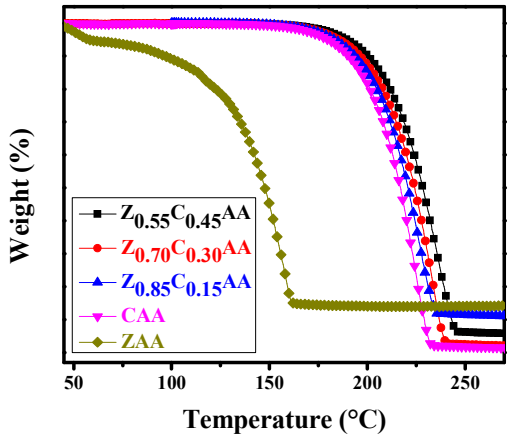

Fig. 11. TGA results of $Z_{0.55}C_{0.45}AA$, $Z_{0.65}C_{0.35}AA$, $Z_{0.80}C_{0.20}AA$, $Z_{0.85}C_{0.15}AA$, $Z_{0.90}C_{0.10}AA$ along with ZAA and CAA.

Conclusions

This study presents a method for the synthesis of bis (acetylacetonato κ-O, O') [zinc (II)/copper (II)]. This complex crystallizes in the monoclinic phase with space group $P2_1/n$. The unit cell dimensions of $Z_{0.7}C_{0.3}AA$ as an example are: a = 10.329(4) Å, b = 4.6947(18) Å, and c = 11.369(4) Å; the angles are: α = 90°, β = 91.881(6)°, and γ = 90°, the volume is 551.0(4) $Å^3$. The TGA results reveal that the compounds lose 3% of their weight at a temperature of between 175~185 °C, proportional to the Cu composition in the complex, implying that the complexes can be used as promising precursors for low temperature synthesis of thin films and nanomaterials with tunable compositions by CVD. The proposed method has several advantages, such as easy work-up process, high yeild of product, and short reaction time. These expensive complexes can be prepared from inexpensive and chemically safe materials with

selective control over the atomic ratio of Cu to Zn in the bimetal complex. Further studies on the application of these compounds are being conducted.

Acknowledgement
The authors acknowledge funding from the National Science Council, Taiwan, under grant NSC 102-2922-L-006-034.

Notes and references

[a]Department of Materials Science and Engineering, National Cheng Kung University, Tainan 70101,Tainan, Taiwan, cpliu@mail.ncku.edu.tw.
[b]Department of Chemical and Materials Engineering, National University of Kaohsiung, Kaohsiung 81148, Taiwan.
[c]Department of Physics, National Cheng Kung University, National Cheng Kung University, Tainan 70101, Taiwan.
[d]Department of Chemistry, Islamic Azad University, Fars Science & Research Branch, P.O. Box 73715-181, Marvdasht, Iran .

Notes and references

1 H. Xu, R. Chen, Q. Sun, W. Lai, Q. Su, W. Huang, X. Liu, *Chem. Soc. Rev.,* 2014, **43**, 3259—3302.
2 V. M. Manikandamathavan, T. Weyhermüller, R. P. Parameswari, M. Sathishkumar, V. Subramanian, B. U. Nair, *Dalton Trans*., 2014, 43, 13018–13031.
3 A. Ghisolfi,K. Y. Monakhov, R. Pattacini, P. Braunstein, X. López, C. d. Graaf, M. Speldrich, J. v. Leusen, H. Schilder, P. Kögerler, *Dalton Trans*., 2014, **43**, 7847–7859.
4 H. T. Ngo, X. Liu, K. A. Jolliffe, *Chem. Soc. Rev*., 2012, **41**, 4928–4965.
5 A. Lauria, R. Bonsignore, A. Terenzi, A. Spinello, F. Giannici, A. Longo, A. M. Almerico, G. Barone, *Dalton Trans*., 2014, **43**, 6108–6119.
6 Z. Zeng, D. Matuschek, A. Studer, C. Schwickert, R. Pottgen and H. Eckert, *Dalton Trans.,* 2013, **42,** 8585-8596.
7 P.J. Hagrman, D. Hagrman, J. Zubieta, *Angew. Chem. Int. Ed.,* 1999, **38**, 2638- 2684.
8 M. Baibarac, I. Baltog, I. Smaranda, M. Scocioreanu, S. Lefrant, *J. Mol. Struct..,* 2011, **985**, 211-218.
9 D. L. Hou, X. J. Ye, H. J. Meng, H. J. Zhou, X. L. Li, C. M. Zhen, G. D. Tang, *Appl. Phys. Lett.,* 2007, **90**, 142502 – 142506.
10 J. Kulesza, B. S. Barrosb, S. A. Júniora. *Coord. Chem. Rev.,,* 2013, **257** , 2192- 2212.
11 M.E. Davis, *Nature.,* 2002, **417,** 813- 821.
12 H. L. Jianga, T. A. Makala, H-C Zhoua. *Coord. Chem. Rev..,* 2013, **257**, 2232- 2249.
13 L. Chow, O. Lupan, G. Chai, H. Khallaf, L.K. Ono, B. R. Cuenya, I.M. Tiginyanu, V.V. Ursaki, V. Sontea, A. Schulte, *Sens. Actuators., 2013,* **189,** 399- 408.
14 F. S. Pomar, E. Martínez, M.F. Meléndrez, E. P. Tijerina, *Nanoscale Res. Lett..*, 2011, **6**, 524- 534.
15 M. S. Raghavan , P. Jaiswal , N. G. Sundaram , S.A. Shivashankar , *Polyhedron* **70** (2014) 188–193
16 A. Gairola, A.M. Umarji, S.A. Shivashankar, *Processing and Properties of Advanced Ceramics and Composites* Edited by Narottam P. Bansal and J. P. Singh Copyright *O* 2009 The American Ceramic Society.
17 A.M. A. Bennett, G. A. Foulds, D. A. Thornton, *Polyhedron.,* 1989**, 8**, 2305- 2311.
18 R. Ferreiraa, M. Silvab, C. Freirea, B. de Castroa, J.L. Figueiredo, *Microporous Mesoporous Mater.*, 2000, **38**, 391-401.
19 H. F. Garces, A. E. Espinal, S. L. Suib, *J. Phys. Chem.,* 2012, **116**, 8465−8474.
20 A.M. EL-Hendawy. *J. Mol. Struct..,* 2011, **995**, 97-102.
21 K. Haga, P. S. Wijesena, H. Watanabe, *Appl. Surf. Sci..,* 2001, **169-170**, 504-507.
22 A.G. Nasibulin, E. I. Kauppinen, D. P. Brown, J. K. Jokiniemi, *J. Phys. Chem.,* 2001, **105**, 11067- 11075.
23 A.Schejn, L.Balan, V.Falk, L.Aranda, G.Medjahdic and R. Schneider, *Cryst Eng Comm.,* 2014,**16**,4494-4500.
24 S. Yokota, Y. Tachi, and S. Itoh, *Inorg. Chem*., 2002, **41**, 1342- 1344.
25 H. Ye, A. Tang, , L. Huang, Y. Wang, C. Yang, Y. Hou, H. Peng, F. Zhang, F. Teng, *Langmuir.,* 2013, **29**, 8728- 8735.
26 R. G. Gonnade, M. M. Bhadbhade, M. S. Shashidhar, *Cryst Eng Comm.*, 2010, **12**, 478-484.
27 G. R. Desiraju, *Angew. chem. Int. Ed. Engl.*, 1995, **34**, 2311- 2327.
28 P. Munshi, B. W. Skelton, J. J. McKinnon, M.A. Spackman, *Cryst Eng Comm.*, 2008, **10**, 197–206.
29 D. Dey, S. Ghosh, D. Chopra, *J Chem Crystallogr.,* 2014, **44**, 131–142.
30 S. Horowitz, R. C. Trievel, *J. Biol Chem.*, 2012, **278**, 41576- 41582.